

## NUMERICAL SIMULATION OF HYPERVELOCITY IMPACTS OF VARIOUSLY SHAPED PROJECTILES WITH THIN BUMPER

M.V. Silnikov<sup>1</sup>, I.V. Guk<sup>1\*</sup>, A.I. Mikhaylin<sup>1</sup>, A.F. Nechunaev<sup>2</sup>, B.V. Rumyantsev<sup>3</sup>

<sup>1</sup>Special Materials Corp., 194044 Bolshoy Sampsonievskiy 28A, St. Petersburg, Russia

<sup>2</sup>St Petersburg University, 199034, University Naberezhnaia 7-9, St. Petersburg, Russia

<sup>3</sup>Ioffe Physical Technical Institute, Russian Academy of Sciences, 194021 Politekhnikheskaia ul. 9,  
St. Petersburg, Russia

\*e-mail: igorguk@ymail.com

**Abstract.** The paper presents a numerical simulation of hypervelocity impacts of variously shaped projectiles with thin bumpers. A numerical model was verified using a full-scale experiment of hypervelocity impact of a sphere with thin aluminum-alloy bumper. Hypervelocity impacts of nonspherical projectiles of different spatial orientation with thin bumpers were also numerically investigated. The investigations show that a hypervelocity impact of a nonspherical projectile advancing with its sharp edge towards the bumper results in a denser debris cloud formation and, therefore, such an impact is more dangerous than any of other considered cases for the spaced protection.

**Keywords:** hypervelocity impact, space debris, non-spherical projectiles, debris clouds, Whipple shields

### 1. Introduction

A quantity of space debris in the near-Earth space is growing in geometric progression [1,2]. Such debris consists of used rocket stages, colliding fragments of spent satellites, etc. Fast and aggressive space development makes protection of space equipment, manned and unmanned space vehicles against hypervelocity impacts in the space very important.

Whipple shields, two or more rigid thin bumpers spaced at a certain distance from each other, are used for protection of the International Space Station against micrometeoroids and man-made debris. The main idea of such spaced multilayer protection is that a hypervelocity projectile breaks and disperses after the interaction with the first bumper. A debris cloud resulted from that impact expands and interacts with the next bumper at a larger area, thus the load intensity of the next bumper significantly decreases [4]. Front bumpers of Whipple shields used at the ISS (International Space Station), about 1-2 mm thickness, are made of heat-strengthened aluminum-alloy, the spaces between the bumpers are filled with layers of woven materials made of aramid and ceramic fibers; the back bumpers are made of aluminum-alloy of about 3-4 mm thickness [5].

For full-scale experimental studies of hypervelocity impacts, projectiles are accelerated mainly by multistage light gas guns. Such studies require many financial and labor expenditures; moreover, with that method of acceleration, it is very hard to achieve a projectile velocity higher than 11-12 km/s. However, velocities of space debris/micrometeoroids impacts can exceed 15 and 30 km/s correspondingly. Therefore, the quantity and quality of full-scale experiments are limited. From another hand, numerical simulations are free from the above-mentioned disadvantages; it is a cost-efficient, visual and

descriptive method of hypervelocity impact investigations. The numerical simulation can result in new geometrical shapes and configurations of the bumpers allowing efficiently absorbing the energy of projectiles of a considerable range of velocities, shapes, and dimensions. Moreover, a shape of debris clouds and their energy, after passing the front bumper, can be studied with a high time resolution, which is very valuable from the scientific point of view. The numerical investigation of the debris cloud dynamics, its propulsion and expansion velocities, mass distribution of debris in the cloud can allow to formulate requirements to a multilayer shield protection more accurately.

## 2. Verification of numerical simulation of hypervelocity impact of spherical projectile with thin bumper

The numerical simulation of a hypervelocity impact of spherical projectiles with a thin bumper was performed using smoothed particles hydrodynamics method [6]. This grid-free Lagrangian method is widely used for describing hypervelocity impact processes; numerical data obtained using this method are in good agreement with known full-scaled experiments [7,8]. Johnson-Cook plasticity and damage equations [9] were applied to describe a behavior of projectiles and bumpers made of aluminum alloys. In the plasticity equation von Mises flow stress  $Y$  depends on strain  $\varepsilon_p$ , strain rate  $\dot{\varepsilon}_p$  and homologous temperature of the material  $T_g$  which depends on temperature  $T$ , initial temperature  $T_0$  and melting temperature  $T_m$ :

$$Y = [A + B\varepsilon_p^n][1 + C \ln \dot{\varepsilon}_p^*][1 - T_g^m], \quad (1)$$

$$T_g = \frac{T - T_0}{T_m - T_0}. \quad (2)$$

A failure criterion – critical strain  $\varepsilon^f$ , is a function of pressure, strain rate and homologous temperature ( $D_1, D_2, D_3, D_4, D_5$ , - empirical coefficients):

$$\varepsilon^f = [D_1 + D_2 e^{D_3 \sigma}][1 + D_4 \ln \dot{\varepsilon}_p^*][1 + D_5 T_g]. \quad (3)$$

The material failure occurs when  $D$  is equal to 1:

$$D = \sum \frac{\Delta \varepsilon}{\varepsilon^f}. \quad (4)$$

For a projectile made of aluminum Al 1100, the equation of state has a form of the Mie–Gruneisen equation assuming linear dependence of pressure  $P$  on internal energy  $E$ . For the shock-compressed material, the pressure was found from:

$$P = \frac{\rho_0 c^2 \mu \left[ 1 + \left( 1 - \frac{\gamma_0}{2} \right) \mu \right]}{[1 - (S_1 - 1)\mu]^2} + \gamma_0 E, \quad (5)$$

where  $c$  – the sound velocity in the material,  $\gamma_0$  – the Gruneisen parameter of the material. For the expanding material the pressure was found from:

$$P = \rho_0 c^2 \mu + \gamma_0 E. \quad (6)$$

For an Al 6061-T6 heat-strengthened aluminum alloy bumper the equation of state was in the form of a linear polynomial ( $C_1, C_2, C_3, C_4$  - coefficients):

$$P = C_1 \mu + C_2 \mu^2 + C_3 \mu^3 + C_4 E. \quad (7)$$

Parameter  $\mu$  is the ratio of material density  $\rho$  to its initial density  $\rho_0$ :

$$\mu = \frac{\rho}{\rho_0} - 1. \quad (8)$$

The approach to plasticity and failure description was made in favor of Johnson-Cook equations because they allow taking into account strain rate and softening temperature including a phase transition. It is important to take into account those factors because at a hypervelocity impact materials of a projectile and a bumper can melt and evaporate. For example, at more than 3 km/s impact velocity interacting aluminum objects partially melt; at more than 7 km/s impact velocity the projectile fully melts [10].

Table 1. Parameters of materials in plasticity and failure equations

| Parameter                          | Unit              | Al 1100            | Al 6061-T6          |
|------------------------------------|-------------------|--------------------|---------------------|
| Initial density, $\rho_0$          | kg/m <sup>3</sup> | 2770               | 2750                |
| Yield stress, $A$                  | Pa                | $4.1 \times 10^7$  | $3.241 \times 10^8$ |
| Strain hardening constant, $B$     | Pa                | $1.25 \times 10^8$ | $1.138 \times 10^8$ |
| Strain hardening coefficient, $n$  |                   | 0.183              | 0.42                |
| Strain rate constant, $C$          |                   | 0.001              | 0.002               |
| Thermal softening coefficient, $m$ |                   | 0.859              | 1.34                |
| Initial temperature, $T_0$         | K                 | 293                | 293                 |
| Melting temperature, $T_m$         | K                 | 893                | 893                 |
| Fracture coefficients, $D_1$       |                   | 0.071              | -0.77               |
| $D_2$                              |                   | 1.248              | 1.45                |
| $D_3$                              |                   | -1.142             | -0.47               |
| $D_4$                              |                   | 0.0097             | 0                   |
| $D_5$                              |                   | 0                  | 1.6                 |

The projectile and the bumper melting and evaporating at a hypervelocity impact increase the protection efficiency. As it is shown in [11], at 7.4 km/s velocity of the copper projectile the copper bumpers are most weight efficient; they have 30% less surface density than the aluminum bumpers with similar protective characteristics. It happens because a copper projectile melts and evaporates most intensively when it interacts with a copper bumper. The chosen equations are widely used for numerical simulations of material impulse loading processes. Therefore, parameters of materials given in Tables 1, 2, 3 for calculations were taken from known sources [12,13].

Table 2. Coefficients in the equation of state for Al 6061-T6

| $C_1$ , GPa | $C_2$ , GPa | $C_3$ , GPa | $C_4$ |
|-------------|-------------|-------------|-------|
| 74.2        | 60.5        | 36.5        | 1.96  |

Table 3. Coefficients in the equation of state for Al 1100

| $c$ , m/s | $S_I$ | $\gamma_0$ |
|-----------|-------|------------|
| 3935      | 1.578 | 1.69       |

The numerical model used in the calculations in this work was verified using the known full-scale experiment. In the paper [14] the experiment of a hypervelocity impact between 5.01-mm ball and 1-mm thick bumper was described. The bumper was made of aluminum alloy Al 6061-T6, and the projectile was made of aluminum Al 1100. The mass of the projectile was 0.18 g. In the full-scale experiment, the impact was at the 90° angle to the bumper surface and the impact velocity was in the range of 4.17-4.33 km/s. The shadowgraphs of the debris cloud forming at the impact and expanding in time were taken at

various moments of time – up to 40  $\mu\text{s}$  after the impact. Therefore, the model parameters were chosen so that the numerical calculation results were in the best agreement with the experimental data.

The hypervelocity impact between a 5.01-mm ball of 0.18g mass and made of Al 1100 and a plane bumper of 1 mm thickness made of Al 6061-T6 was numerically simulated. The impact was at 4.19 km/s velocity and perpendicular to the bumper surface. All simulations were performed in 3D formulation.

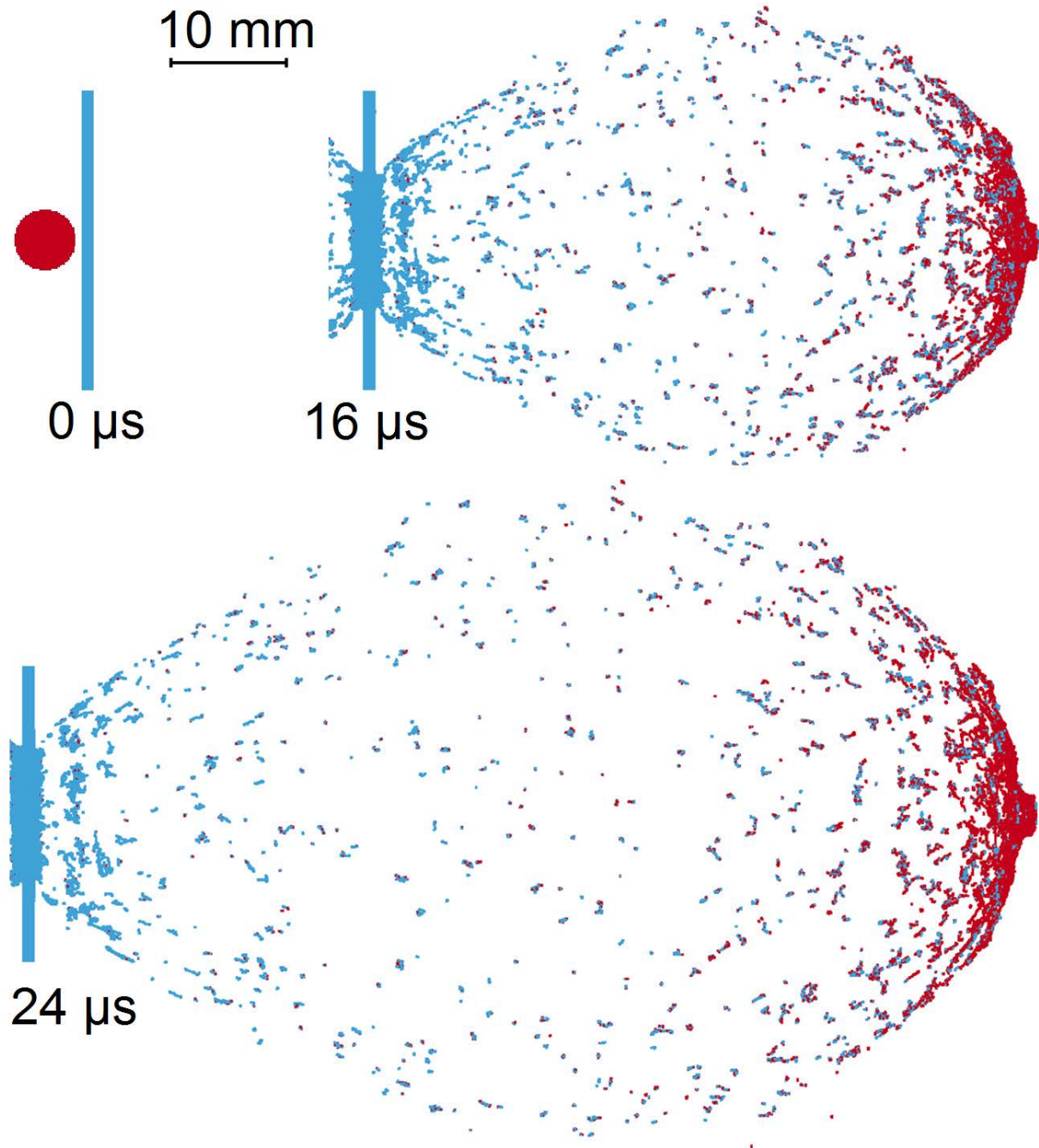


**Fig. 1.** Debris cloud formed 16  $\mu\text{s}$  and 24  $\mu\text{s}$  after the impact, side view. Spherical Al 1100 projectile with velocity of 4.19 km/s, Al 6061-T6 bumper with thickness of 1 mm

Figure 1 presents images (side views) of the debris clouds resulted from the impacts at 16  $\mu\text{s}$  and 24  $\mu\text{s}$  moments of time and initial state of the problem (0  $\mu\text{s}$ ). The numerical calculation is in good agreement with the full-scale experimental data. The main mass of

debris is concentrated in a head part of the cloud. The images obtained in both the full-scale and numerical experiments show the characteristic “bulge” in the head part (vanguard) of the debris cloud. The numerical simulation allows distinctly distinguishing materials of the projectile and the bumper and track dynamics of the bulge generation and development frame-by-frame with  $10^{-8}$  s time resolution.

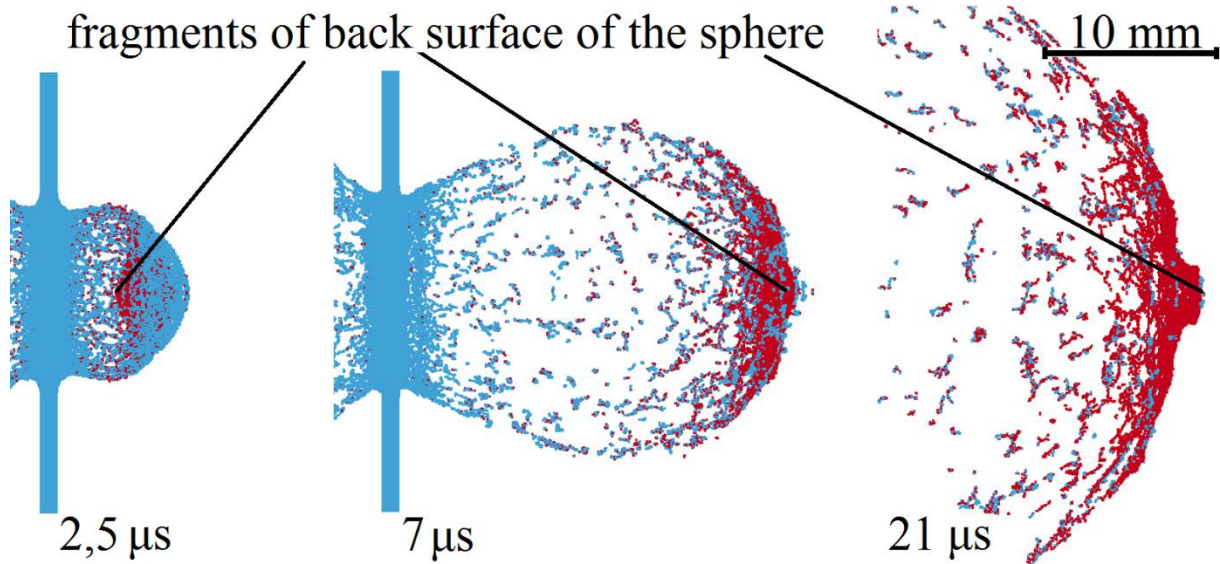


**Fig. 2.** "Bulge" development in the debris cloud vanguard. Positions of fragments, belonging to the back surface of the sphere are pointed out. Spherical Al 1100 projectile with mass of 0.18 g and velocity of 4.19 km/s, Al 6061-T6 bumper with thickness of 1 mm

The numerical calculations show that the bulge in the vanguard of the debris cloud consists of projectile particles gathered into a dense group and advancing along the impact trajectory. At 2.5  $\mu$ s (Fig. 2) the projectile debris has formed rather a dense group of the shape reminding the initial shape of the projectile. That group has a mixed phase composition; the debris are in both liquid and solid phases there. In time, the solid fragments from the remote surface of the projectile are outrunning the main mass of the debris in the vanguard and forming the bulge in the head part of the cloud. It happens because these fragments are moving with higher longitudinal velocity than the bumper debris and other debris of the projectile. The similar bulge was observed in [15,16] under alike initial conditions – impact velocity, projectile diameter and bumper thickness, but the projectile and the bumper were made from a different grade of aluminum. By all appearance, for such a bulge formation the projectile material should have less density and ultimate strength than the bumper material. Under that condition, 4.19 km/s impact velocity is not enough for complete melting of the projectile and the remote part of it remains in the solid phase [17]. The evaporated and melted material is expanding rather evenly with the cloud advancement, whereas the solid particles remain on the impact axis. Exactly those particles are the biggest threat for the spaced multilayer bumper protection.

At 16  $\mu$ s moment of time the cloud length/diameter ratio in the widest part is 1.58 mm (the numerical calculation) and 1.53 mm (the full-scale experiment), the error is less than 3.5%. At 24  $\mu$ s moment the length/diameter ratio is 1.58 mm (numerical calculation) and 1.59 mm (the full-scale experiment), the error is less than 0.5%. With inaccuracy of the geometric dimensions measuring taken into the account, it is fair to conclude that the numerical calculation error in comparison with the full-scale experiment is less than 4%. From the equality of the cloud's geometric dimensions (length and diameter) at the same moments of time, we can conclude that relations of the expansion velocity in longitudinal and



transverse directions are equal in both full-scale and numerical experiments. The diameter values of the crater forming on the bumper are also in satisfactory agreement. In the numerical calculation, it is 11.3 mm, in the full-scale experiment – 11 mm. The vanguard cloud velocity is 3.74 km/s in the calculation and 3.8 km/s in the full-scale experiment. In general, the numerical simulation has been performed with satisfactory accuracy, therefore, the selected approach and the material parameters can be used for investigation of hypervelocity impacts between projectiles and bumpers of other configuration.

### 3. Simulation of non-spherical projectiles impact with thin bumper

A spherical shape of the projectile is a simplification, in real life space debris colliding with space vehicles can be of various shapes. Numerical calculations allow investigating hypervelocity impacts of projectiles of various shape and spatial orientation and comparing differences and characteristics of debris clouds formed in various cases. With the help of the verified model, a hypervelocity impact of a cylindrical projectile (its diameter is equal to its length) on a thin bumper has been simulated. The impact velocity, projectile material (Al 1100), bumper material (Al 6061-T6), bumper thickness (1 mm) and projectile mass (0.18 g) are identical to the verified case. Therefore, results of impacts of projectiles with the same kinetic energy but of various shapes can be compared; and it is possible to determine the distinctive features of debris clouds formed as a result of the impacts of various projectiles.

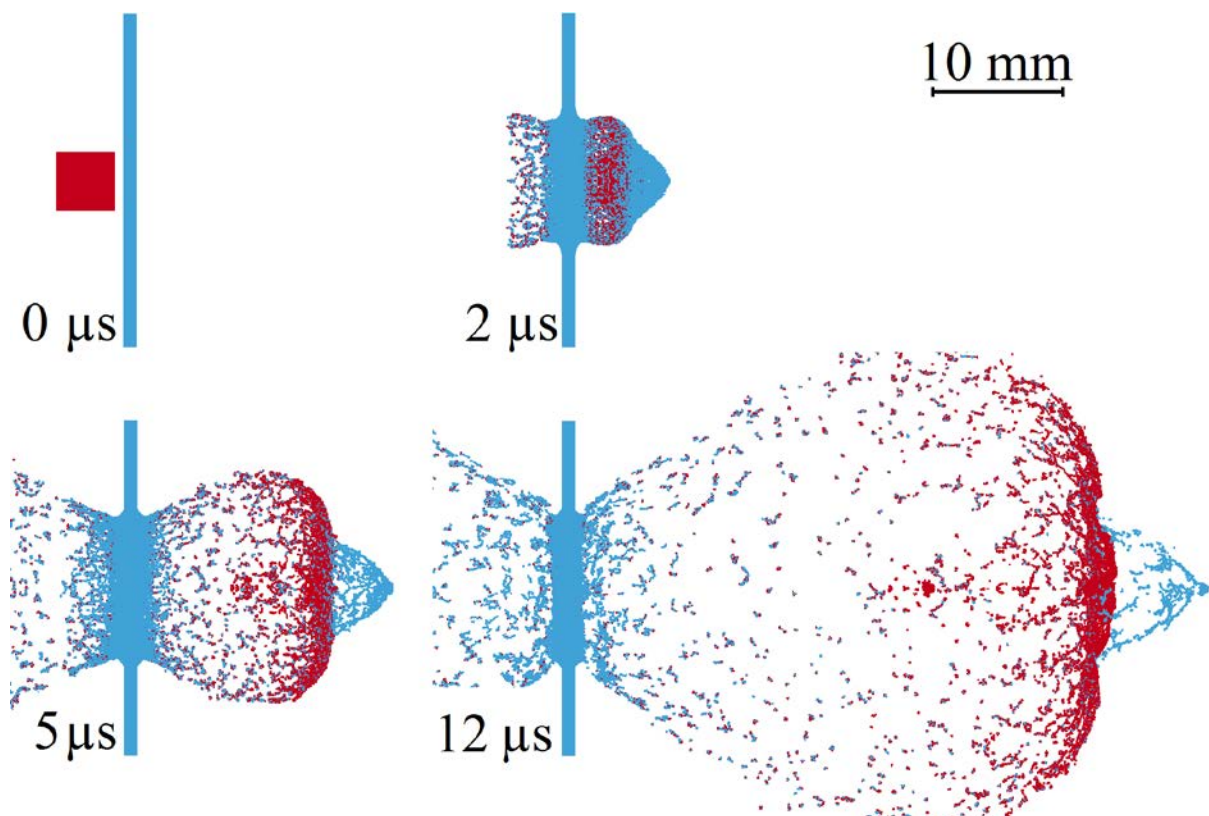


**Fig. 3.** The debris cloud formed after the impact of 0,18 g cylindrical Al 1100 projectile with 1mm thin Al 6061-T6 bumper at various moments of time. Side view. Projectile velocity – 4.19 km/s, projectile mass – 0.18 g, bumper thickness – 1 mm. (Note, that in the side view of three-dimensional problem cylinder with its diameter equal to length looks like a cube)

At the initial stage of the debris cloud formation, the symmetric outer cone of particles of rear bumper surface is formed on the impact axis (Fig. 3). In time, the outer cone is expanding and a dense debris group, rather evenly distributed on the cloud front surface, is

following it. The debris mass advancing along the impact axis is approximately 20% out of the initial projectile mass. The debris vanguard on the front surface is expanding evenly with the cloud advancement. The debris cluster on the impact axis following the cone is less subjected to the expansion and preserves practically all its mass during the simulated period (0-12  $\mu$ s). Thus, that cluster is the most dangerous part of the debris cloud for the spaced bumper protection against the cylindrical projectile impact.

Similar debris cloud characteristics – the cluster on the impact axis and the leading cone were obtained experimentally in [18]. In that hypervelocity impact experiment, cylindrical projectile was made of Al 2024-T4 and 2 mm thin bumper was made of Al 6061-T6. Most likely, the leading debris cone is formed due to the bumper material spallation. In that case, the initial stage of the bumper destruction has a shock-wave nature induced by shock waves generation in the bumper resulted from the plane shock and rarefaction waves following the shock wave front.

#### **4. Study of cubic projectile orientation effect on results of impact with thin bumper**

Axial-symmetric projectiles (cylinders, balls) can be accelerated to space velocities (4-5 km/s and more) by light gas guns. It is simpler to study hypervelocity impacts of projectiles without axial symmetry (projectiles of arbitrary shapes that are closer to real life space debris) numerically. For the extreme case study 3D calculations of a cubic shape projectile with its face and edge orientated toward a thin bumper have been performed.

Initial conditions, mass and velocity of cubic projectiles, projectiles' and bumpers' materials, coincide with those used in the calculations of impacts between the spherical and cylindrical projectiles and the thin bumper. Two cases of hypervelocity impacts have been studied: in the first case, the cube face was parallel to the bumper surface; in the second case, the projectile edge was oriented to the bumper surface.

The development dynamics of the debris cloud in both simulated cases (Fig. 4) has been studied and compared. When the cube impacts by its face, a formed debris cloud is similar to the one resulted from a cylindrical projectile of the same mass and with a diameter equal to the length. Both clouds have similar characteristics– the leading cone and the dense group of the projectile particles with the 20% out of the initial projectile mass in the vanguard of the debris cloud. The characteristic cloud dimensions at 12  $\mu$ s moment of time, such as a length without the leading debris cone and a diameter in the widest part, are approximately equal. The cloud length without the bumper debris cone is 38.5 mm, which is approximately the same as the diameter in the widest part (38 mm).

We observe a different picture when the cube impacts by its edge (Fig. 4). In this case, most of the projectile fragments (more than 50% of the initial mass) are concentrated in the dense group on the impact axis. The diameter of the cloud in the widest part reduces to 24 mm at 12  $\mu$ s moment of time. In case of the cube face impact, the angle of the debris dispersion is about 30 degrees to the impact trajectory; debris are evenly dispersed on the cloud front surface and form a small compaction on the impact axis. In the case of the cube edge impact, the resulted debris cloud is narrower and oblong. The angle of the debris dispersion is 20 degrees to the impact trajectory; the projectile debris forms a dense group in the center. In this case, the cloud vanguard velocity is 3,9 km/s, which is 7% higher than in the case of the face impact. Such reduction in the debris dispersion area and an increase of the debris velocity reduces the efficiency of spaced multilayer protection. The leading cone of debris is absent due to a constant applied load that prevents the spallation of the rear bumper surface.

The results of calculations show that at hypervelocity impacts of projectiles of nonspherical, cylindrical or cubic, shapes with a protective structure consisting of two spaced bumpers, the load intensity on the second bumper cannot be significantly reduced by increasing the distance between the bumpers. The best solution is to fill the space between the

bumpers with ballistic materials or with some liquid or gaseous medium [19]. In case of a spherical projectile, projectile and bumper debris are dispersed on the cloud vanguard rather evenly. Such a cloud is expanding to all directions uniformly, therefore increasing the gap between the bumpers we increase the load area. However, in the case of a nonspherical projectile, a dense debris group is formed on the impact axis; this group does not expand considerably in time, and it interacts with the second bumper on the same area independently on the distance between the bumpers. This phenomenon is visualized better in case of the cubic edge impact on the bumper; when more than a half of the initial projectile mass remains on the impact axis. It could be caused by a shorter lifetime of shock waves and fewer pressure values developing in nonspherical projectiles [20]. As a result, the projectile destruction is less intensive; larger fragments are formed that can be seen in the case of the cube sharp edge impact.

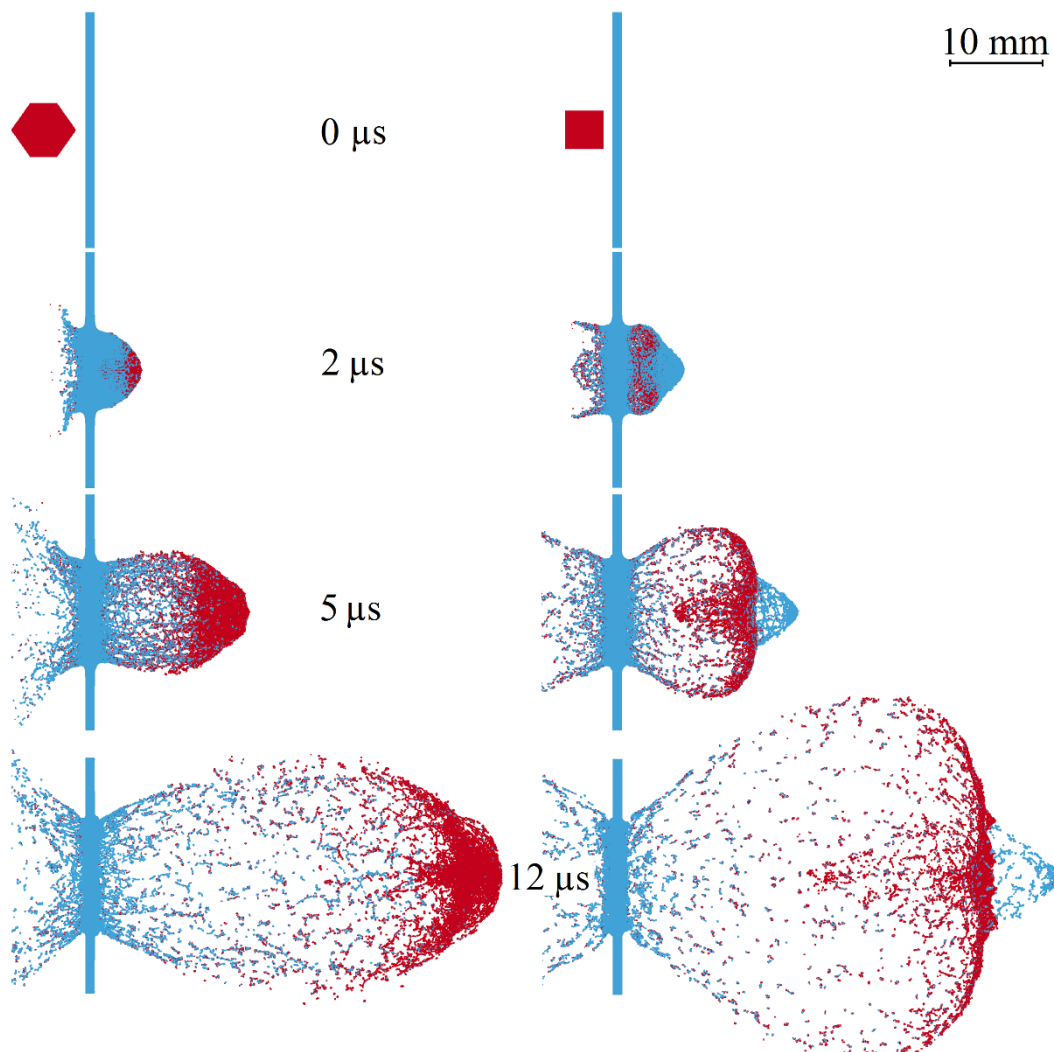


**Fig. 4.** Comparison of the debris clouds formed in various moments of time due after hypervelocity impacts of cube Al-1100 projectiles of different spatial orientations with thin Al 6061-T6 bumpers. Side view. Projectile velocity – 4.19 km/s, projectile mass – 0.18 g, bumper thickness – 1 mm. (Note, that in the side view of three-dimensional problem cube oriented with its edge towards the bumper looks like a hexagon)

Comparing images of the debris clouds formed in all cases considered, it is fair to conclude that at a hypervelocity impact of nonspherical particle by their sharp edge with a spaced bumper protection the penetration of the second bumper is most probable. Such a



configuration, two bumpers at a certain distance from each other, is much less efficient in protection against space debris of nonspherical shape. Thus, the conclusion made in [21] is confirmed.

## 6. Conclusions

In general, all results obtained by the calculations are in good agreement with known experimental data. Thus, the model used in this work can be applied to further studies on hypervelocity impacts. The numerical model describing a process of a hypervelocity impact of a spherical projectile on a thin bumper has been verified. Based on the similarity between known experimental results and obtained numerical data, we can conclude that the method applied, equations and material parameters are valid.

The performed calculations show that at a hypervelocity impact of an aluminum ball on a bumper made of a heat-strengthened aluminum alloy, a "bulge" is formed in the cloud vanguard on the impact axis. It consists of material of the remote surface of the projectile. At the hypervelocity face impact of a cylindrical or cubic projectile, a leading cone is formed due to the spallation of rear surface of the bumper.

The calculations of a nonspherical projectile orientation effect on the debris cloud formation have been performed. Two boundary cases – cubic face and cubic sharp edge impacts, have been considered. In case of the face impact, the angle of disperse is higher than in case of the edge impact, and the debris are rather evenly dispersed on the cloud vanguard with small thickness (bulge) on the impact axis. When the cube impacts by its edge, the cloud formed is much narrower, the disperse angle is only 75% of the angle in the face impact case. The debris are dispersed on the vanguard unevenly, more than 50% of the initial projectile mass is concentrated in the dense group on the impact axis, and the cloud vanguard advancement velocity is 10 % higher.

Reduction of the debris dispersion area and an increase of their velocity cause reduction of the bumper protection efficiency. The calculations of hypervelocity impacts of nonspherical projectiles using the verified model show that penetration of two spaced bumpers is most probable in the case when a cubic projectile impacts the bumper by its sharp angle, which is verified by known experimental data. At hypervelocity impact between a nonspherical, cylindrical or cubic projectile (with its sharp edge) and a two spaced bumper protection, the load intensity of the second bumper cannot be significantly reduced by increasing the distance between the bumpers, because the main part of fragments in the debris cloud is propagating along the impact axis.

**Acknowledgements.** *This work was financially supported by Russian Foundation for Basic Research, №18-08-00487/18.*

## References

- [1] Smirnov NN, Nazarenko AI, Kiselev AB. Modelling of the space debris evolution based on continua mechanics. *Space Debris*. 2001;473: 391-396.
- [2] Smirnov NN, Kiselev AB, Kondratyev KA, Zolkin SN. Impact of debris particles on space structures modeling. *Acta Astronautica*. 2010;67(3-4): 333-343.
- [3] Whipple FL. Meteorites and space travel. *The Astronomical Journal*. 1947;52: 131.
- [4] Zukas JA, Nicholas T, Swift HF, Greszczuk LB, Curran DR. *Impact Dynamics*. Florida: Krieger; 1992.
- [5] Christiansen EL, Crews JL, Williamsen JE, Robinson JH, Nolen AM. Enhanced meteoroid and orbital debris shielding. *International Journal of Impact Engineering*. 1995;17(1-3): 217-228.

- [6] Liu MB, Liu GR. *Smoothed Particle Hydrodynamics A Meshfree Particle Method*. Singapore: World Scientific Publishing; 2003.
- [7] Hiermaier S, Konke D, Stilp AJ, Thoma K. Computational simulation of the hypervelocity impact of Al-spheres on thin plates of different materials. *International Journal of Impact Engineering*. 1997;20(1-5): 363-374.
- [8] Poniaev SA, Kurakin RO, Sedov AI, Bobashev SV, Zhukov BG, Nechunaev AF. Hypervelocity impact of mm-size plastic projectile on thin aluminum plate. *Acta Astronautica*. 2017;135: 26-33.
- [9] Johnson GR, Cook WH. A constitutive model and data for metals subjected to large strains, high strain rates and high temperature. In: *Proceedings 7th International Symposium on Ballistics*. 1983. p.541-547.
- [10] O'Connor B. *Handbook for limiting orbital debris, NASA Handbook 8719.14*. Washington DC: National Aeronautics and Space Administration; 2008.
- [11] Rumiantsev BV, Mikhaylin AI. Phase transition effect on efficiency of screen protection against elongated hyper-velocity projectiles. *Acta Astronautica*. 2017;135: 15-20.
- [12] Veisi B, Narooei K, Zamani J. Numerical investigation of circular plates deformation under air blast wave. *Iranian Journal Materials Forming*. 2016;3(1): 12-26.
- [13] Lesuer DR, Kay GJ, LeBlanc MM. *Modelling large-strain, high-rate deformation in metals*. CA (US): Lawrence Livermore National Lab.; 2001.
- [14] Ke FW, Huang J, Wen XZ, Ma ZX, Liu S. Test study on the performance of shielding configuration with stuffed layer under hypervelocity impact. *Acta Astronautica*. 2016;127: 553-560.
- [15] Chi RQ, Pang BJ, Guan GS, Yang ZQ, Zhu Y, He MJ. Analysis of debris clouds produced by impact of aluminum spheres with aluminum sheets. *International Journal of Impact Engineering*. 2008;35(12): 1465-1472.
- [16] Poormon KL, Piekutowski AJ. Comparison of cadmium and aluminum debris clouds. *International Journal of Impact Engineering*. 1995;17(4-6): 639-648.
- [17] Piekutowski AJ. Characteristics of debris clouds produced by hypervelocity impact of aluminum spheres with thin aluminum plates. *International Journal of Impact Engineering*. 1993;14(1-4): 573-586.
- [18] Piekutowski AJ. Debris clouds generated by hypervelocity impact of cylindrical projectiles with thin aluminum plates. *International Journal of Impact Engineering*. 1987;5(1-4): 509-518.
- [19] Smirnov NN, Kiselev AB, Smirnova MN, Nikitin VF. Space traffic hazards from orbital debris mitigation strategies. *Acta Astronautica*. 2015;109: 144-152.
- [20] Schoneberg WP, Bean AJ, Darzi K. *Hypervelocity impact physics*. 1991.
- [21] Morrison RH. *A preliminary investigation of projectile shape effects in hypervelocity impact of a double-sheet structure*. 1972.